Virchows Arch A (1987) 410:281–294

Virchows Archiv A

Some ultrastructural features of the myocardial cells in the hypertrophied human papillary muscle

Helge Dalen,[1] Thorvald Sætersdal,[2] and Svein Ødegården[2]

[1] Laboratory of Clinical Electron Microscopy and
[2] Cellular Cardiology Research Group, Institute of Anatomy, University of Bergen, Norway

Summary. An ultrastructural study using various electron microscopical techniques has been conducted on biopsy material from the hypertrophied papillary muscle of the human heart. About 75% of the myocardial cells were classified as hypertrophic with diameters ranging from 15 μm to 53 μm. The increased cell diameter appeared to be the result of an elevated amount of mitochondria and contractile material. The hypertrophied myocytes displayed a general ultrastructural organization in many ways similar to that of the normal sized myocytes. However, the former cells were characterized by focal deposits of excess laminar coat material and abnormal Z-band patterns as well as of multiple intercalated discs. The preferential sites for the production of new sarcomere elements appeared to be in the subsarcolemmal and intercalated disc regions. Adjacent myocardial cells were interconnected by collagen bundles, and, by an elaborate collagen-fibril-microthread-granule lattice. The surface folds were linked to each other by surface cables, which probably constituted a separate category of extracellular material of unknown function. Intramembranous particles were abundant in the sarcolemma proper but scarce in the membranes of the sarcoplasmic vesicles. Such particles were also observed in the lipofuscin granular membrane and in the membranes surrounding the lipid droplets. A framework of transverse cytoskeletal filaments interconnected the Z-bands of adjacent myofibrils and anchored the contractile material to the sarcolemma as well as to the nucleus. A large and lobulated nucleus containing well developed nucleoli together with an abundance of sarcoplasmic free and membrane-attached ribosomes, were interpreted as morphological signs of enhanced synthetic activity in the hypertrophied cell. Degenerative phenomena on the other hand were confined to lysosomal degeneration of worn-out cell constituents that were manifested by the numerous lysosomes and aggregates of lipofuscin granules. Abnormal Z-band patterns as seen in the present material were interpreted as an initial stage in the formation of new contractile elements.

Key words: Human heart – Papillary muscle – Myocardial hypertrophy – Ultrastructure

Offprint requests to: H. Dalen, Laboratory of Clinical Electron Microscopy, University of Bergen, 5016 Haukeland Hospital, Norway

Introduction

Since the advent of transmission electron microscopy (TEM) the subcellular organization of the myocardial tissue has been investigated in a number of mammalian species. The extensive body of information accumulated on this subject has recently been reviewed by Sommer and Johnson (1979) and Forbes and Sperelakis (1983, 1984).

While there is a lack of ultrastructural information on the completely normal human myocardium, numerous electron microscopical studies have been conducted on tissue from the hypertrophied human heart (Ferrans et al. 1972; Kajihara et al. 1973; Maron et al. 1975a, b; Sætersdal et al. 1976; Maron and Ferrans 1978; Jones and Ferrans 1979; Schaper et al. 1981; Kawamura 1982). Such investigations have almost exclusively been based on biopsy material from various parts of the ventricular wall, while ultrastructural studies of the hypertrophied papillary muscle are rare (Kaijhara et al. 1973; Caulfield and Borg 1979).

In a previous study we emphasized the advantage of using various electron microscopical techniques for characterizing the subcellular organization of the hypertrophied human papillary muscle (Dalen et al. 1986). The present communication

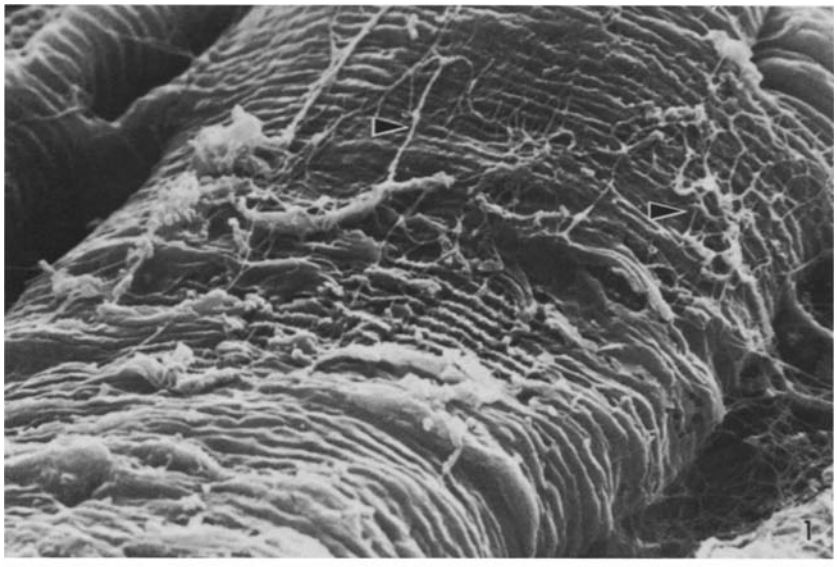

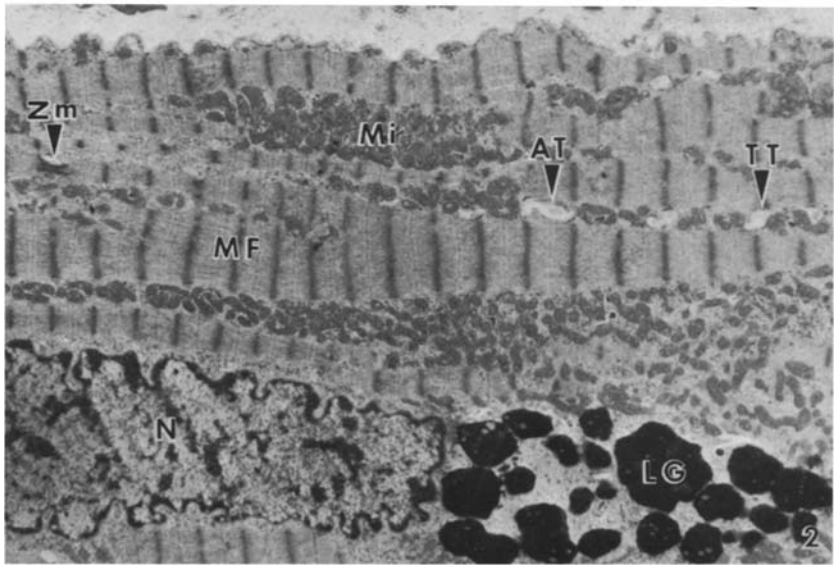

Fig. 1. A scanning electron micrograph of the human papillary muscle cell from cryofractured material. The scalloped surface of the branched myocyte is encased by a network of collagen bundles (*arrowheads*) of varying caliber. × 5,000

Fig. 2. A longitudinal section of a conventionally prepared papillary muscle fiber. The striated myofibrils (*MF*) are separated by numerous pleomorphic mitochondria (*Mi*) arranged in rows or large aggregates. Note the abnormal Z-band material (*Zm*). Both transverse (*TT*) and axial (*AT*) tubules are few in number and irregularly distributed. Lipofuscin granules (*LG*) are accumulated in the nuclear pole sarcoplasm. The nuclear envelope of the centrally located nucleus (*N*) is characterized by numerous indentations. × 3,000

contains additional ultrastructural informations concerning this particular tissue using the same techniques.

Material and methods

Biopsy material of the human papillary muscle was obtained during open heart surgery of two adult patients suffering from mitral stenosis. Immediately after surgical removal the tissue was placed in ice-cold Hank's balanced salt solution, cut into small pieces and divided into four groups. Each group was processed for electron microscopical studies according to one of the different methods described below.

For conventional TEM the tissue was fixed overnight in 2% glutaraldehyde followed by 1 h in 1% OsO_4. Both fixatives were made up in 0.1 M cacodylate buffer (pH 7.2) with 0.1 M sucrose (Ericsson et al. 1978) and applied under ice-cold conditions. After standard dehydration, Epon-embedding and polymerization thick (1 μm) and thin sections were cut on a Reichert ultramicrotome. Light microscopy was conducted on thick sections stained with toluidine blue, while thin sections were contrasted with uranyl acetate and lead citrate and examined in a Philips 300 TEM operated at 60 kV.

Another group of tissue was, after glutaraldehyde-fixation as above, subjected to *en bloc* staining with Cu-Pb citrate solution for 24 h at 4° C (Thiéry and Bergeron 1976). Postfixation for another 24 h with ice-cold 1% OsO_4 was followed by conventional dehydration, plastic embedding, polymerization and ultramicrotomy. Thick and thin sections without further contrasting were studied in a Philips 300 TEM operated at 80 kV. Stereoscopic pictures of the thick sections were obtained by tilting the goniometer stage plus and minus 6° from the zero position between two successive exposures.

Scanning electron microscopy (SEM) was carried out on cryofractured material prepared according to the method described by Dalen et al. (1978). In brief, tissue fixed in glutaraldehyde as above was embedded in paraffin, frozen in liquid N_2, cryofractured, deparaffinized with xylol and critical point dried. After mounting and coating with gold, the fractured material

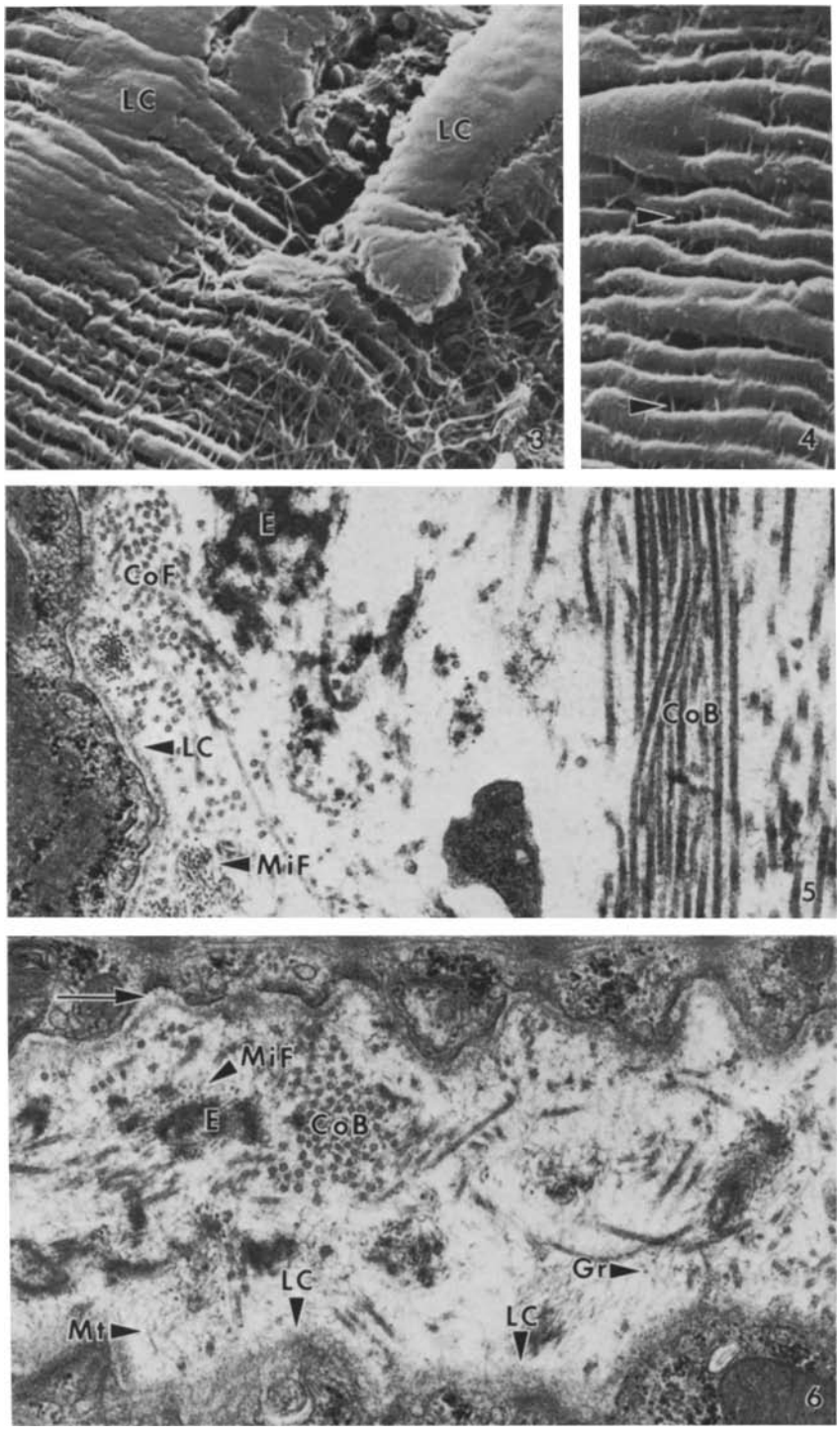

Figs. 3–4. SEM of cell surface details. In some regions a markedly thickened laminar coat (*LC*) conceals the underlaying surface details. Longitudinally oriented surface cables (*arrowheads*) interconnect the ridges of the transversely folded cell surface. Fig. 3, ×5,000; Fig. 4, ×6,000

Figs. 5–6. Transmission electron micrographs illustrating the diversity of structures of which the connective tissue is composed. Numerous microfibrils (*MiF*) are frequently seen in association with elastin (*E*). An elaborate network of collagen fibrils (*CoF*), microthreads (*Mt*) and granules (*Gr*) interconnect the lateral surfaces of adjacent myofibers. The branching microthreads attach to the laminar coat (*LC*) which again is anchored by fine fibrils (*arrow*) to the plasma membrane. Note the thickened laminar coat in Fig. 6. Both micrographs ×30,000

was viewed in a Philips 500 SEM using an accelerating voltage of 25 kV. Stereo scanning electron micrographs were taken by tilting the goniometer stage 10° between two successive exposures.

The material of the last group was processed for freeze-fracture replicas. Thirty minutes fixation in 2% buffered glutaraldehyde at 4° C was followed by 30 min impregnation with 30% cacodylate-buffered glycerole and mounted on gold specimen holders. Tissue quench frozen in melting Freon 22 was fractured in a Balzer's freezefracture apparatus, replicated with carbon/palladium according to standard techniques and examined in a Philips 300 TEM at 80 kV.

Results

Thick sections of the biopsy material examined in the LM revealed that about 25% of the myofibers

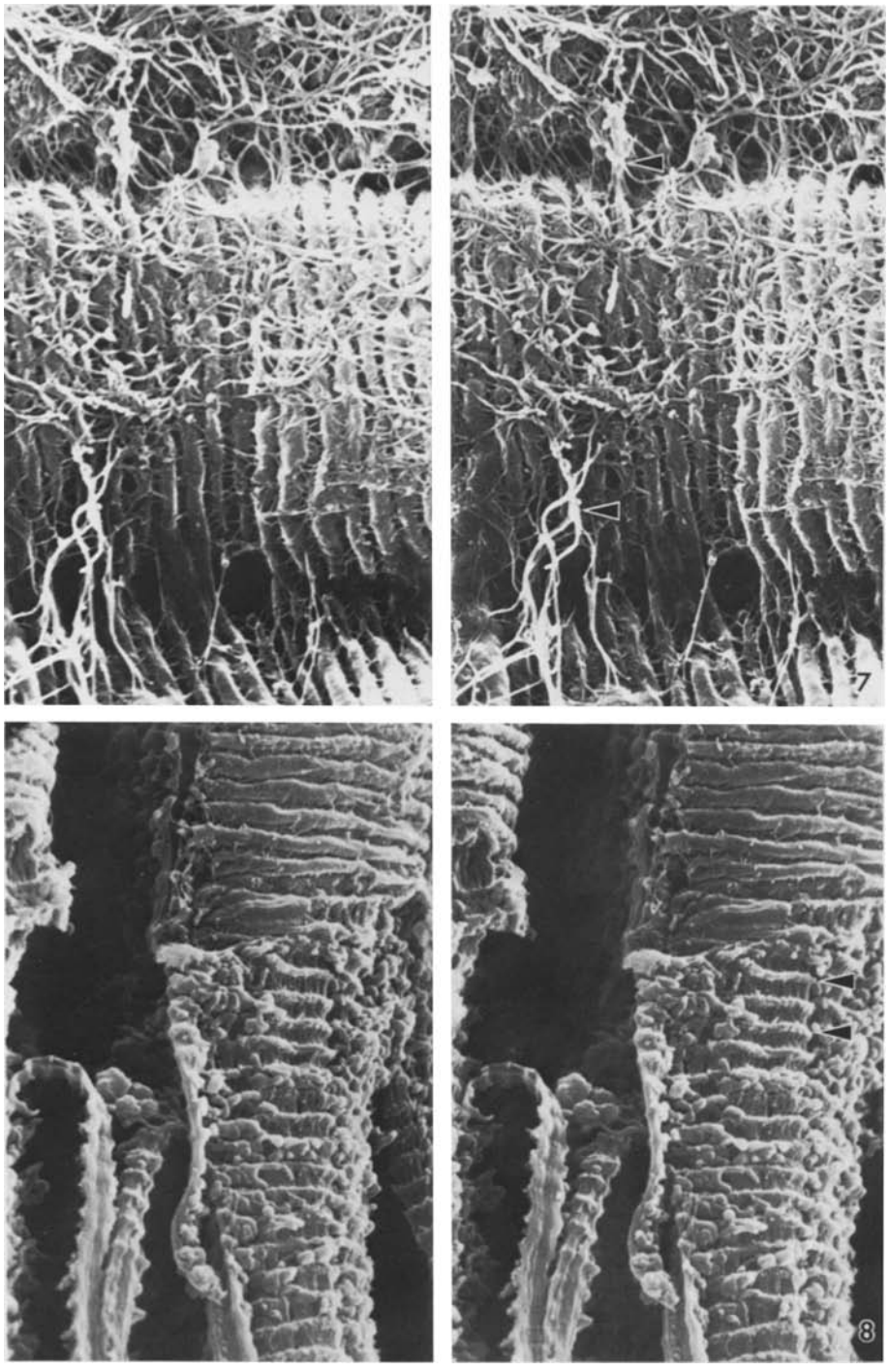

Fig. 7. Stereo scanning electron micrographs (10° tilt) of cryofractured material demonstrating the three-dimensional organization of the collagenous weave and struts (*arrowheads*) surrounding and interconnecting myocardial cells. ×4,500

Fig. 8. Another stereo-pair of the same material as depicted in figure 7. In the upper part of the micrographs the folded sarcolemma has been left intact, while in the lower part the subsarcolemmal cell interior has been exposed. Numerous pleomorphic mitochondria are situated adjacent to the surface of the crossbanded contractile material. Transverse tubules (*arrowheads*) in some places are superimposed on top of the elevated Z-bands. ×4,500

had transverse diameters ranging from 10 μm to 15 μm, which corresponds to the values reported for normal human myocardial cells (Jones and Ferrans 1979). The remaining heart muscle cells had diameters ranging from 15 μm to 53 μm. Although the fiber diameter had increased in the latter cells, mainly due to an elevated number of contractile elements and mitochondria, the majority of the hypertrophied cells revealed a general subcellular organization which in most respects appeared similar to that of the normal sized myocytes. However, a number of quantitative and qualitative alterations in the various cell organelles were noted.

The branching heart muscle cells were encased by a weave of connective tissue in which the collagen fibrils, organized into bundles or struts, made

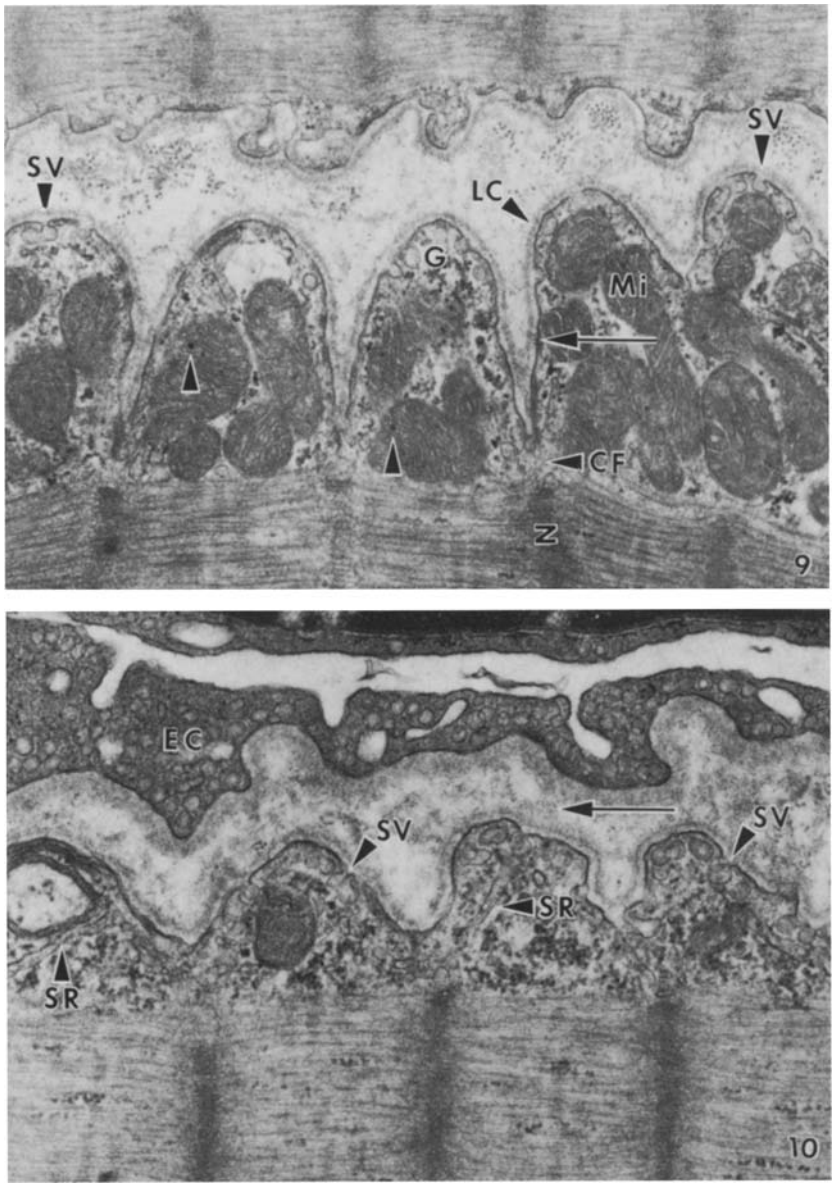

Figs. 9–10. The ultrastructure of the peripheral portion of the myocardial cell as it appears in thin sections of conventionally processed tissue. The sarcolemmal folds contain various cell components including mitochondria (*Mi*), sarcoplasmic reticulum (*SR*) and glycogen particles (*G*). Note the presence of a few intramitochondrial electron-dense particles (arrowheads). The sarcolemma which is attached to the underlying Z-bands (*Z*) by cytoskeletal filaments (*CF*), is invaginated by abundant sarcolemmal vesicles (*SV*). Note that these vesicles contain an electron-dense material similar to that of the laminar coat (*LC*). The latter structure is attached to the plasma membrane by fine fibrils (*arrow*, Fig. 9). Strands of the laminar coat material (*arrow*, Fig. 10) connect the highly vesiculated capillary endothelial cell (*EC*) with the muscle fiber. Both micrographs × 30,000

lateral connections between adjacent myofibers (Figs. 1, 7). Examination in the TEM displayed another group of intercellular linkages which were composed of an elaborate collagen fibril-microthread-granule lattice (Figs. 5, 6). The microthreads intermingled with the laminar coat material which in turn was anchored to the plasma membrane by thin fibrils. The external cell surface displayed regions with a markedly thickened laminar coat (Figs. 3, 6, 14). Other members of the extracellular skeletal framework included elastin and microfibrils (Figs. 5, 6).

In the contracted muscle fiber the sarcolemma, which is regularly attached to adjacent Z-bands (Fig. 9), displayed a pronounced scallopped pattern (Figs. 1–4, 7–11). The surface folds were interconnected by surface cables which were arranged in parallel with the long axis of the myocytes (Fig. 4). The folds contained various cell organelles including mitochondria, free- and junctional sarcoplasmic reticulum (SR) and glycogen (Figs. 9–12).

Both the free cell surface and its internal extensions (T-system) exhibited numerous small inpocketings (Figs. 9–12). These caveolae, or sarcolemnal vesicles, which often appeared in clusters communicated with the extracellular space through narrow necks. The vesicles contained an electron-dense material similar to that of the laminar coat. Intramembranous particles, which in freeze fracture preparations were a common feature of the

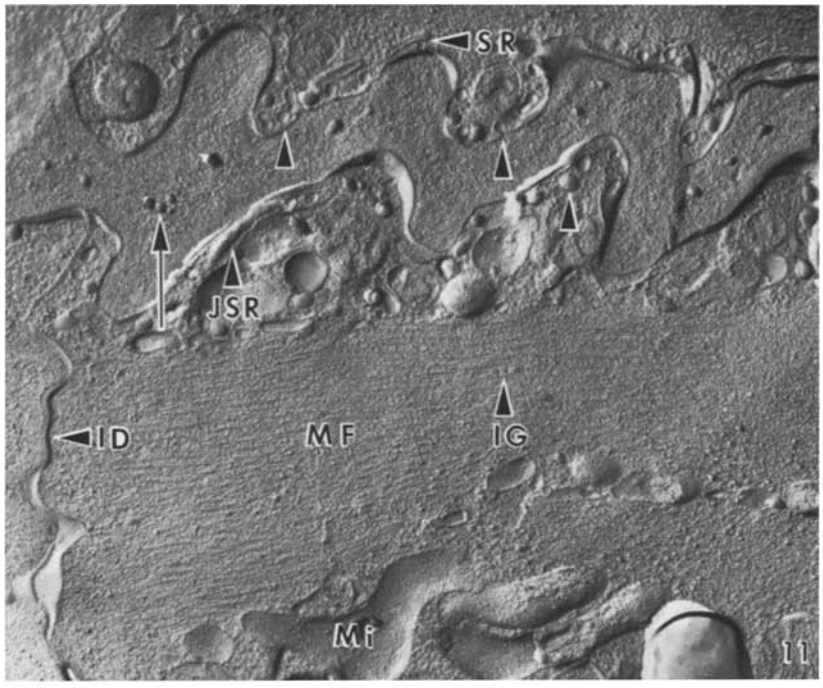

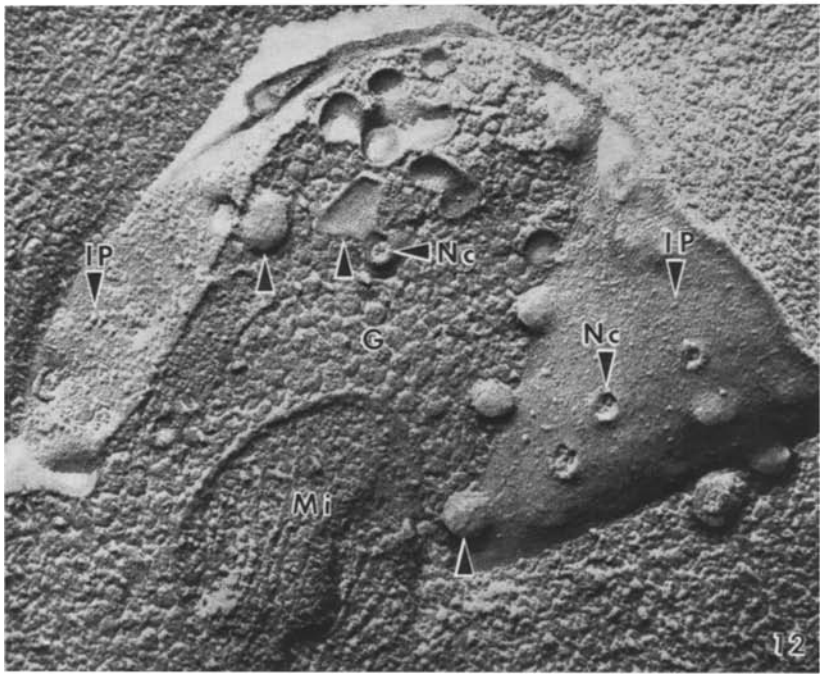

Figs. 11–12. Freeze fracture replicas of the peripheral sarcoplasm and intercellular space. Mitochondria (*Mi*), glycogen particles (*G*), profiles of the sarcotubular system (*SR*) and abundant sarcolemmal vesicles (*arrowheads*) are readily recognized. While the cell surface proper contains numerous intramembranous particles (*IP*), the sarcolemmal vesicular membrane is almost completely devoid of such structures. In the intercellular space the connective tissue appears as a network of thin fibers or bundles (*arrow*). *JSR*, junctional *SR*. MF, myofibrils. *IG*, interfilamentous glycogen. *ID*, intercalated disc. *Nc*, sarcolemmar vesicular neck. Fig. 11, ×25,000; Fig. 12, × 60,000

plasmalemma proper, were only rarely observed in the caveolar membrane (Fig. 12).

Generally, the myofibers were arranged in parallel arrays interspersed by rows or large aggregates of the pleomorphic mitochondria (Fig. 2). Focally some subsarcolemmal regions contained polyribosomes and elements of forming contractile material that occurred together with thickened Z-bands and various abnormal patterns of the Z-band material (Figs. 13, 14).

Multiple intercalated discs were commonly present (Fig. 15). These structures consisted of two or more transverse intercalated discs arranged in parallel and separated by one to a few sarcomeres. Extensive accumulations of an electron-dense material similar to that of the Z-bands were located

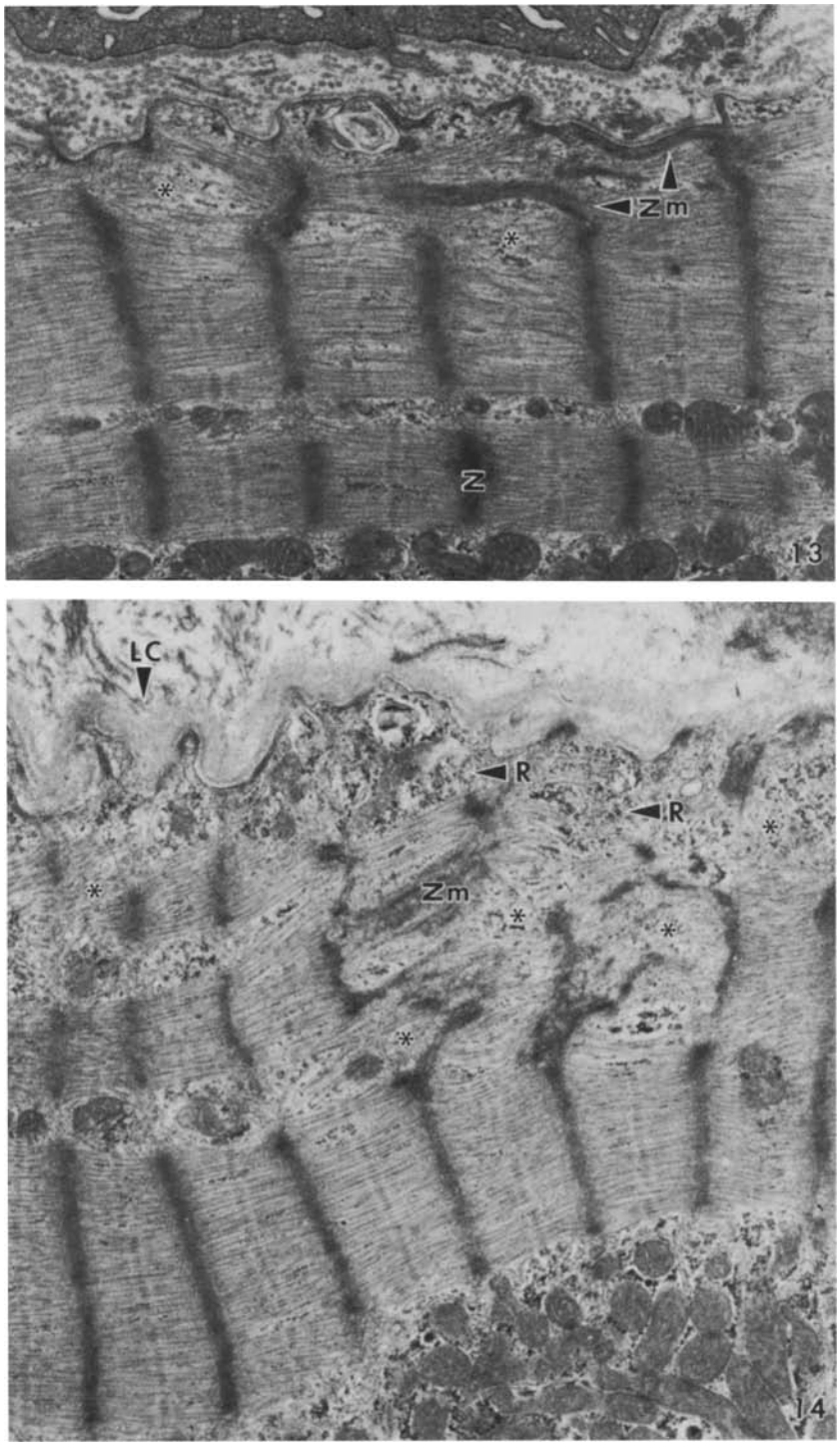

Figs. 13–14. Transmission electron micrographs of regions with thickened Z-bands (*Z*) and Z-band material (*Zm*) arranged in various abnormal patterns. These regions also contain clusters of ribosomes (*R*) and forming myofilaments (*asterisks*). Note the markedly thickened laminar coat (*LC*, Fig. 14). Both micrographs × 20,000

on the sarcoplasmic aspect of the intercalated discs. Some of this material extended deep into adjacent sarcomeres. Numerous ribosomes and forming myofilaments were frequently observed in these regions.

Bundles of cytoskeletal filaments occurred in conventionally prepared thin sections (Figs. 9, 16) and in cryofractured tissue (Fig. 17). These filaments constituted a transverse framework interconnecting the Z-bands of adjacent myofibrils and binding the Z-bands to the sarcolemma and the nuclear envelope. Microtubules, which are the other cytoskeletal constituent, were not observed.

The hypertrophied myocardial cells were cha-

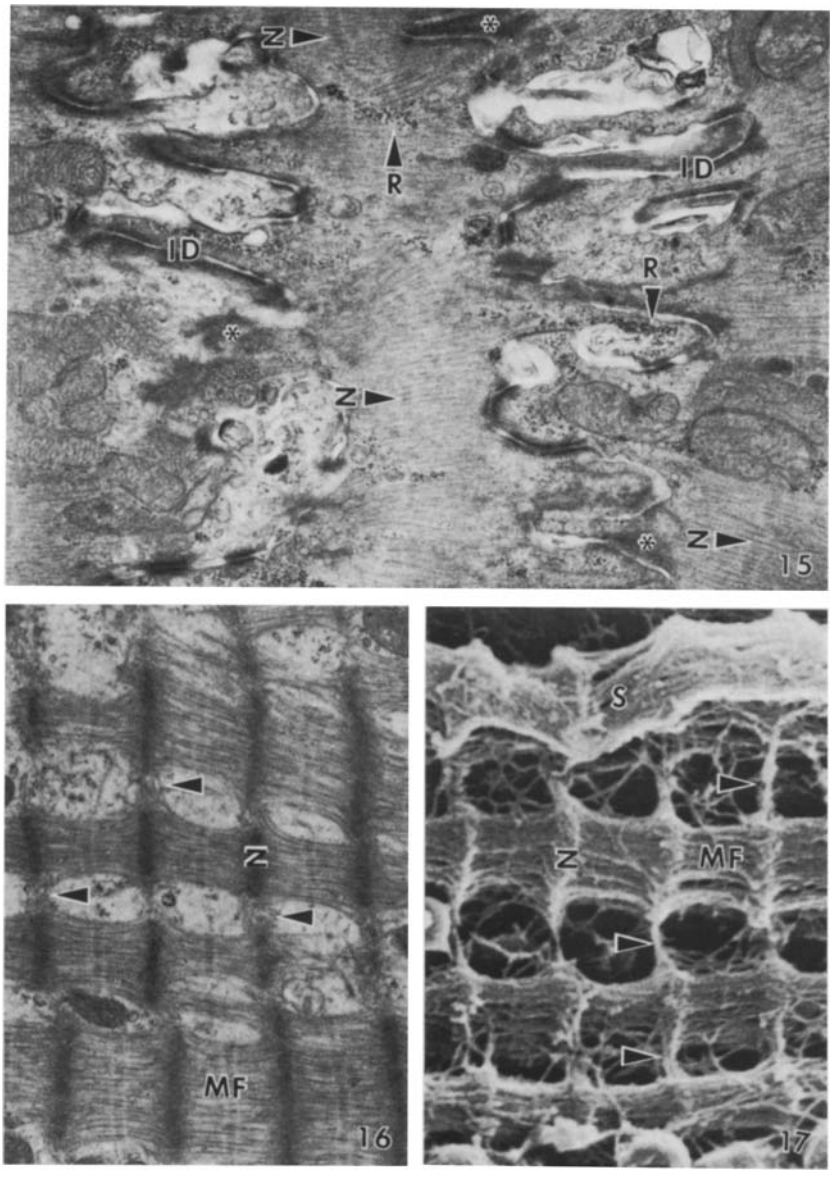

Fig. 15. An example of a multiple intercalated disc consisting of two parallel discs separated by a single immature sarcomere. Note the forming Z-bands (*Z*), clusters of ribosomes (*R*) and electron-dense material (asterisks) adjacent to the intercalated discs (*ID*), ×20,000

Figs. 16–17. The transverse network of cytoskeletal filaments (arrowheads) interconnecting Z-bands (*Z*) of adjacent myofibrils (*MF*) as it appears in conventional thin sections (Fig. 16), and, in cryofractured tissue (Fig. 17). The cytoskeletal filaments are also connected to the sarcolemma (*S*). Both micrographs ×15,000

racterized by large and lobulated nuclei (Fig. 18). Numerous nuclear pores penetrated the deeply indented nuclear envelope (Fig. 19). Thin sections frequently revealed one or two large nucleoli (Figs. 18, 20). The heterochromatin was deposited on the inner nuclear envelope or scattered throughout the nucleoplasm.

The nuclear pole sarcoplasm contained a number of various cell constituents, including abundant pleomorphic mitochondria, numerous free or membrane-attached ribosomes (RER), glycogen particles, extensive Golgi apparatus, lysosomes, myelin figures, lipofuscin precursor granules (LPG) and lipofuscin granules (LG) (Figs. 18, 21–25). The RER was continuous with the outer nuclear membrane (Fig. 22), and the lysosomes were frequently seen adjacent to the Golgi saccules (Fig. 24). The LPG were characterized by their crystalline inclusions (Fig. 23), while the LG contained lipid droplets of variable diameters together with an electron-dense heteromorphic material (Fig. 24). Freeze-fracture preparations of the LG revealed that the granular membrane as well as the membranes surrounding the lipid droplets contained intramembranous particles (Fig. 25).

Discussion

According to Maron et al. (1975b), hypertrophied myocardial cells can be divided into two main

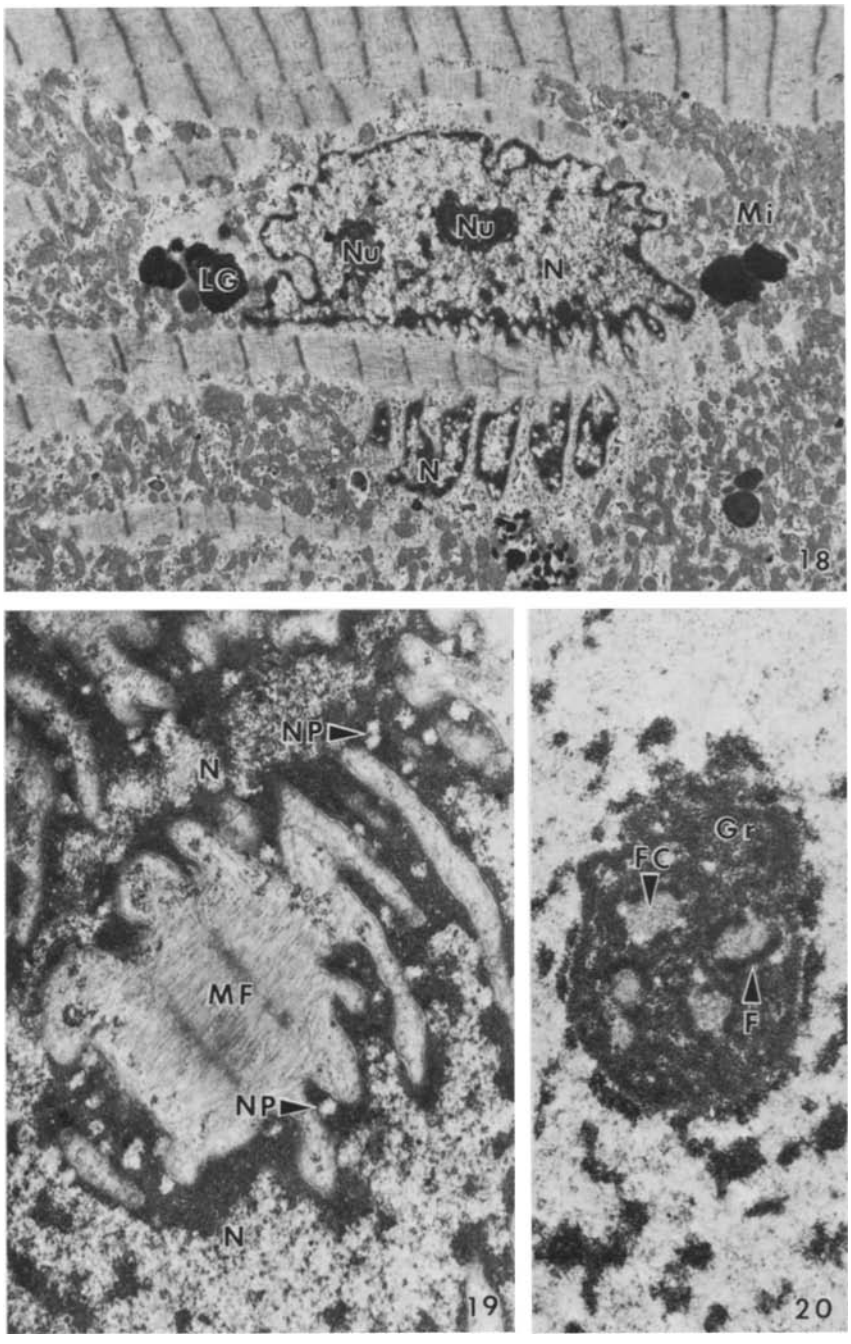

Figs. 18–20. Transmission electron micrographs showing various ultrastructural features of the hypertrophied cell nucleus. The large and lobulated nucleus (*N*) is surrounded by a deeply indented envelope, which is perforated by numerous nuclear pores (*NP*). Thin sections commonly reveal one or two large nucleoli (*Nu*) with a well developed substructure (Fig. 20), consisting of a granular component (*Gr*), a fibrillar component (*F*) and a fibrillar centre (*FC*). The electron-dense heterochromatin is deposited on the inner nuclear membrane or scattered throughout the nucleoplasm. Note the accumulation of pleomorphic mitochondria (*Mi*) and lipofuscin granules (*LG*) in the perinuclear region. MF, myofibril. Fig. 18, ×7,500; Fig. 19, ×20,000; Fig. 20, ×15,000

groups, namely, those without evidence of degeneration and those with degenerative alterations.

In the present material the majority of the hypertrophied cells displayed a normal distribution and organization of the various cell organelles, although a number of qualitative alterations were noted. Thus, focal abnormalities such as extensive deposits of laminar coat material and abnormal Z-band patterns were occasionally seen. The latter structures occurred in regions where additional contractile material appeared to be produced. Structures representing lysosomal degeneration of worn-out cell organelles were predominately located in the perinuclear region.

Correlative scanning and transmission electron miroscopic studies are especially useful for defining the ultrastructure of the fibrous interstitial network. The organization of the connective tissue in the micrographs shown here is in main accordance with a previous study of the hypertrophied

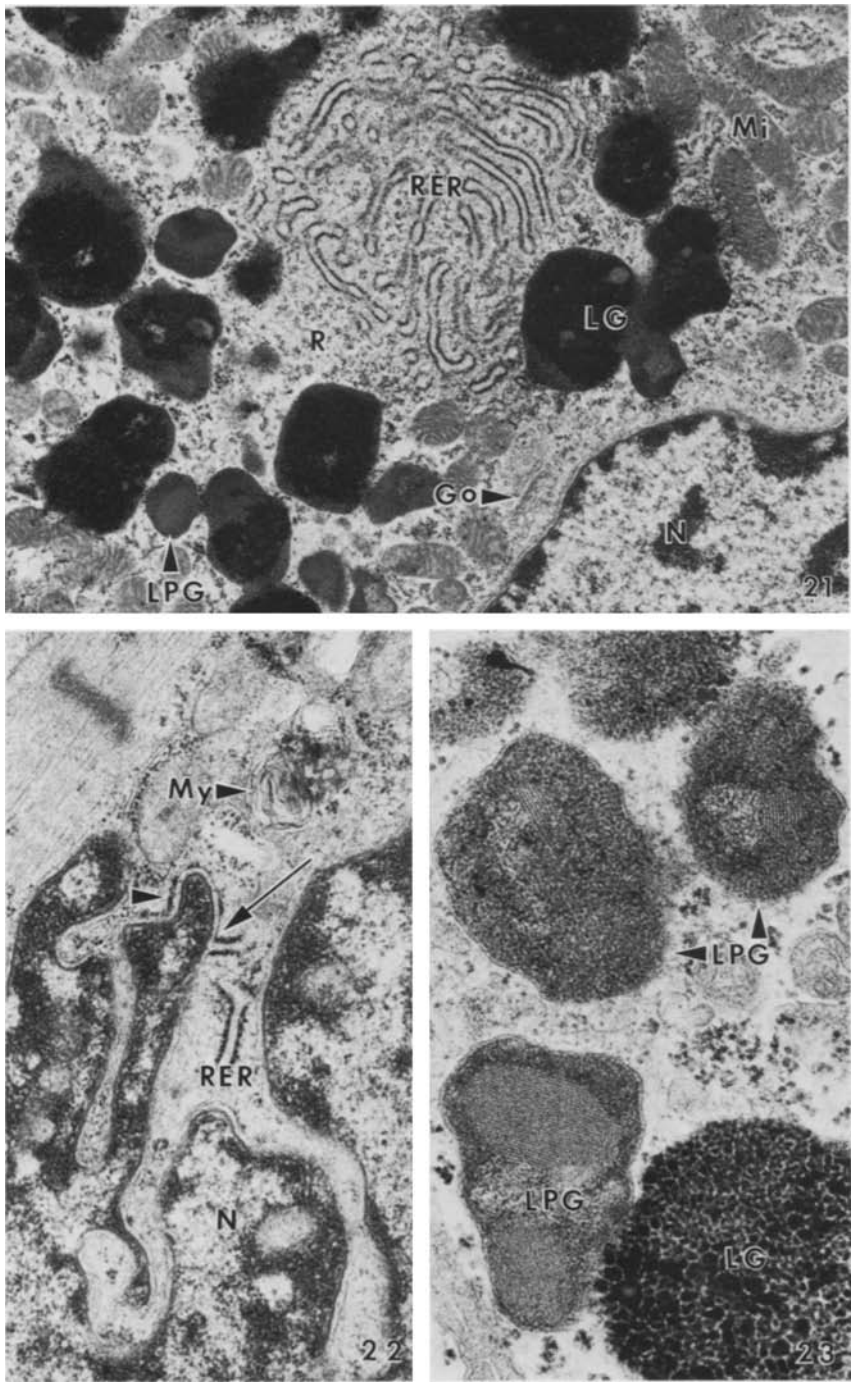

Figs. 21–24. Transmission electron micrographs of conventionally processed tissue displaying various perinuclear organelles including mitochondria (*Mi*), free mono- and polyribosomes (*R*), rough-surfaced endoplasmic reticulum (*RER*), Golgi complex (*Go*), lysosomes (*Ly*), lipofuscin precursor granules (*LPG*) and lipofuscin granules (*LG*). The LPG are characterized by their contents of lattice-like structures. Note the deeply invaginated nuclear membrane, the continuity of the RER with the outer nuclear envelope (*arrow*), and the short segment of the latter structure studded with ribosomes (*arrowhead*). *N*, nucleus. *L*, lipid droplet, *My*, myelin figure. Fig. 21, ×15,000; Fig. 22, ×30,000; Fig. 23, ×50,000; Fig. 24, ×25,000

human papillary muscle (Caulfield and Borg 1979). Qualitatively, the composition of the interstitial material is also very similar to that described in the normal heart of rodents (Caulfield and Borg 1979; Borg and Caulfield 1979; Robinson and Winegrad 1981; Borg et al. 1982). Based on extensive light and electron microscopical studies, Robinson et al. (1983) have proposed an architectural model according to which the connective tissue has a dual physiological function. In addition to maintaining mechanical stability it is also crucial for assisting the normal functioning of myofibers and capillaries during the cardiac cycle. Thus, ultrastructural knowledge of the morphological organization of the connective tissue in biopsy material may be important for the judgement of the pathophysiological state of the myocardial cells.

Although surface cables have been reported on both heart and skeletal muscle cells of various mammalian and non-mammalian species (Oren-

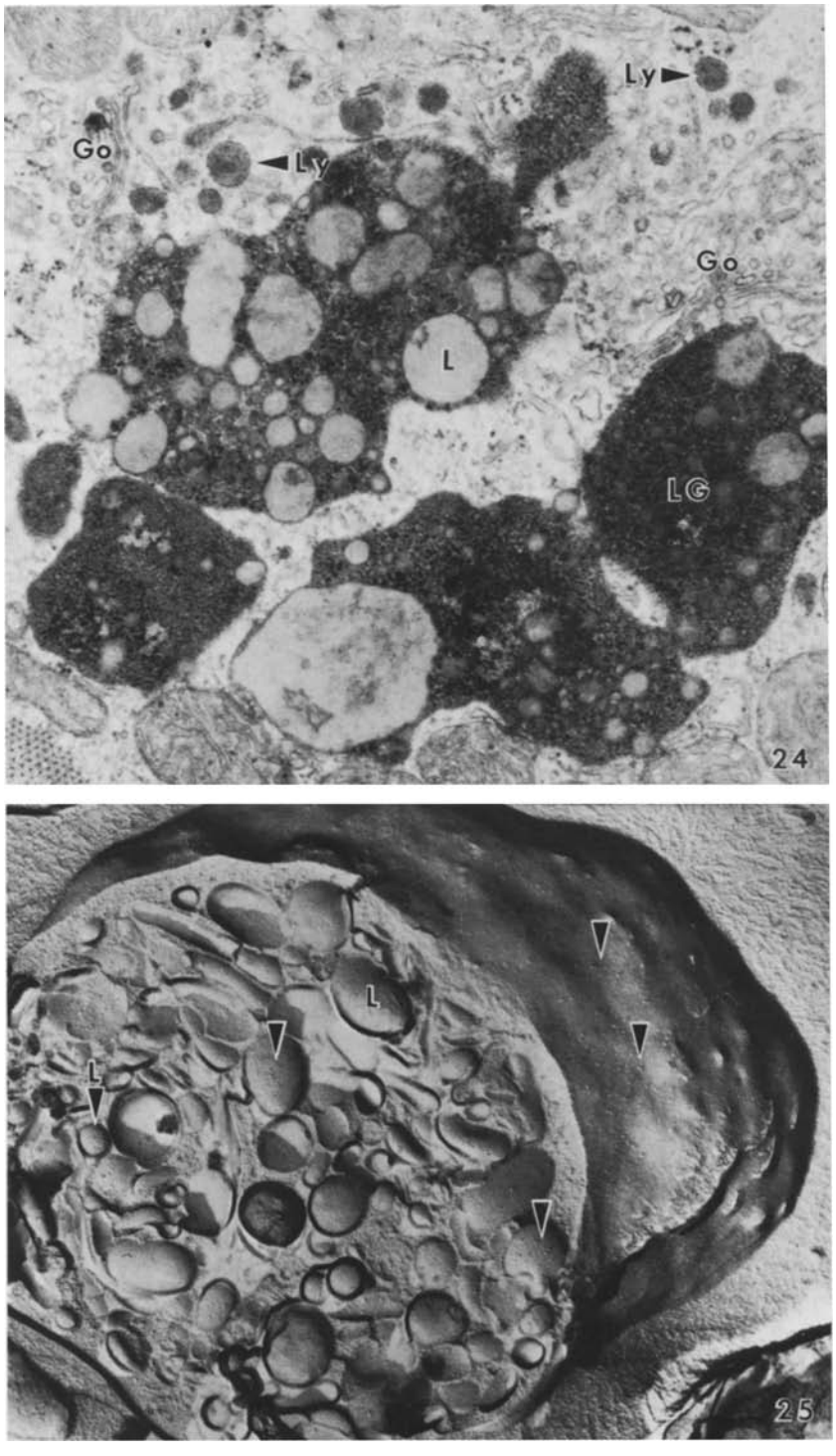

Fig. 25. Freeze fracture replica of a lipofuscin granule displaying lipid droplets (*L*) of varying sizes. Note the presence of intermembraneous particles (*arrowheads*) in the membranes surrounding the lipid droplets as well as in the membrane of the lipofuscin granule itself. ×25,000

stein et al. 1980; Caceci et al. 1981), SEM of the present material has for the first time reported the presence of such structures on the human myocardial cell surface. The extent to which these cables are an integral part of the interstitial fibrillar network remains to be explored. It is possible that they provide the morphological basis for restricting the diastolic compliance of the heart muscle (Orenstein et al. 1980). Also, it seems reasonable to assume that the deposition of excess laminar coat material, as observed in the present tissue, interferes with the normal functioning of the surface cables.

Preparation of freeze fracture replicas is necessary in order to study the distribution of intramembranous particles. The observation here that the

density of such particles is strikingly much higher in the plasmalemma proper than in the caveolar membrane is in accordance with the findings in other mammals (Gabella 1978; Levin and Page 1980) and may reflect functional differences in the two membranes. Levin and Page (1980) have discussed the possibility that the intramembranous particles are instrumental in the transmembrane ion flow and that the caveolae represent sites of reduced flow.

It is also possible that the caveolae might represent reservoirs of cell membrane to be recruited during stretching of the myocardial cell and thus act as stretch receptors (Prescott and Brightman 1976). However, the observation that these surface specializations contain an electron-dense material favours the hypothesis that they are instrumental in renewing the laminar coat material (Carrascal et al. 1981).

The majority of the myofibers in the material shown here had compensated for the increased mechanical work load by producing additional contractile material and by increasing the mitochondrial mass. Morphological evidence for cell hyperactivity in hypertrophied myofibers has been found in the large and distorted nucleus as well as in the enlarged nucleoli (Cluzeaud et al. 1984). Furthermore, the presence of abundant free and membrane-attached ribosomes as well as widened Z-bands have been interpreted as a morphological manifestation of active synthesis of new functional components (Goldstein et al. 1974). It has been postulated that the accumulations of Z-band material serve as templates for the organization of new sarcomeres (Bishop and Cole 1969; Legato 1970; Legato et al. 1984), although other reports do not lend support to this view (Colborn and Carsey 1972; Maron and Ferrans 1974). Still others advocate that the anomalous accumulations of Z-band material represent a nonspecific response on the part of the muscle to a variety of etiologic factors (Ferrans et al. 1975; Sætersdal et al. 1976). Although abnormal Z-band patterns have also been regarded as a degenerative phenomenon (Maron et al. 1975b), the presence of such structures in regions with an apparent production of new sarcomere material as shown in this study, may suggest that they represent a developmental stage in sarcomerogenesis during hypertrophy.

The preferential sites for such activities in the hypertrophied cells appear to be the subsarcolemmal regions and the regions adjacent to the intercalated discs. It has also been suggested that the latter regions may be involved in the reinforcement of the lateral connections between adjacent cells as a response to the increased mechanical tensions (Laks et al. 1979; Maron and Ferrans 1973; Adomian et al. 1974).

The framework of transversly oriented cytoskeletal filaments that interconnect Z-bands of adjacent myofibrils and that also anchors the Z-bands to the sarcolemma and the nuclear membrane (Ferrans and Roberts 1973) is thought to be a crucial structure for keeping the contractile elements in proper alignment during the cardiac cycle (Lazarides 1980). While such filaments may be difficult to identify in conventional thin sections, they are readily displayed in cryofractured material where the myofibrils have been artificially separated (Dalen et al. 1983) as a result of tissue shrinkage after critical point drying (Boyde 1978). It is also believed that the T-tubules, including their connections with the Z-bands (Forbes and Sperelakis 1976) in concert with elements of the SR at the Z-band level (i.e. Z-tubules and junctional SR), contribute to the transverse stabilization of the heart muscle cell (Forbes and Sperelakis 1980).

Also the microtubules have been thought to serve a cytoskeletal function in myocardial cells (Goldstein and Entman 1979). The lack of microtubules in the present tissue is undoubtedly a preparative artefact since it has been shown that these organelles depolymerize upon exposure to low temperatures (Behnke 1967; Roth 1967; Tilney and Porter 1967). Fixation with cacodylate buffered glutaraldehyde is also unfavourable for their preservation (Luftig et al. 1977).

Further, it has been shown that experimentally induced myocardial hypertrophy in animals results in an enhanced population of lysosomes (Breisch 1982; Breisch et al. 1984) and that lipofuscin granules are numerous in biopsy material of the human hypertrophied heart (Maron et al. 1975b). The observation that they occur together with lysosomes and lipofuscin proccursor granules (Van Noorden et al. 1971) has been reconfirmed in this material. It has been suggested that the lipofuscin granules represent the end product of lysosomal degeneration of mitochondria and other cell organelles (Travis and Travis 1972). This view has been supported by a more recent study on the origin of lipofuscin (Koobs et al. 1978).

During hypertrophy, the myocardial cells have to replace worn out and degenerated mitochondria as well as compensate for the increased mechanical load by producing more mitochondria. A possible mechanism leading to the enhancement of the mitochondrial mass will be discussed elsewhere (Dalen 1987).

Acknowledgements. We are indebted to Dr. Hogne Engedal, Department of Cardiac Surgery, Haukeland Hospital, for kindly supplying us with the biopsy material. The technical

assistance of Mr. Jakob Røli, Mrs. Anne Marie Sandsbakk Austarheim and Miss Brynhild Haugen, and the secretarial help of Mrs. Aud Lie-Nilsen is greatly acknowledged. We are also grateful to Professor Paul Scheie, Texas Lutheran College, and Professor Melvyn Lieberman, Duke University Medical Center, USA, for their helpful discussion and comments during preparation of this manuscript.

References

Adomian GE, Laks MM, Morady F, Swan HJC (1974) Significance of the multiple intercalated disc in the hypertrophied canine heart. J Molec Cell Cardiol 6:105–109

Behnke O (1967) Some possible practical implications of the lability of blood platelet microtubules. Vox Sang 13:502–507

Bishop SP, Cole CR (1969) Ultrastructural changes in the canine myocardium with right ventricular hypertrophy and congestive heart failure. Lab Invest 20:219–229

Borg TK, Caulfield JB (1979) Collagen in the heart. Texas Rep Biol Med 39:321–333

Borg TK, Sullivan T, Ivy J (1982) Functional arrangement of connective tissue in striated muscle with emphasis on cardiac muscle. Scan Electr Microsc IV:1775–1784

Boyde A (1978) Pros and cons of critical point drying and freeze drying for SEM. Scan Electr Microsc II:303–314

Breisch EA (1982) Myocardial lysosomes in pressure-overload hypertrophy. Cell Tissue Res 223:615–625

Breisch EA, White FC, Bloor CM (1984) Myocardial characteristics of pressure overload hypertrophy. A structural and functional study. Lab Invest 51:333–342

Caceci T, Orenstein JM, Bloom S (1981) Surface cables of vertebrate muscle cells. Scan Electr Microsc III:115–123

Carrascal E, Leon L, Alexandre C (1981) Caveolae system in the myocardium of the rat. Morphol Normal y Patol Sec A 5:121–128

Caulfield JB, Borg TK (1979) The collagen network of the heart. Lab Invest 40:364–372

Colborn GL, Carsey jr E (1972) Electron microscopy of the sinoatrial node of the squirrel monkey Saimiri sciureus. J Molec Cell Cardiol 4:525–536

Cluzeaud F, Perrenec J, De Amoral E, Willenium M, Hatt PY (1984) Myocardial cell nucleus in cardiac overloading in the rat. Eur Heart J 5 (Suppl. F):271–280

Dalen H (1987) An ultrastructural study of myocardial cell mitochondria in the hypertrophied human papillary muscle. Virchows Archiv [Pathol Anat] (submitted)

Dalen H, Myklebust R, Sætersdal TS (1978) Cryofracture of paraffin-embedded heart muscle cells. J Microsc 112:139–151

Dalen H, Scheie P, Myklebust R, Sætersdal T (1983) An ultrastructural study of cryofractured myocardial cells with special attention to the relationship between mitochondria and sarcoplasmic reticulum. J Microsc 131:35–46

Dalen H, Ødegården S, Sæterdal TS (1987) The application of various electron microscopic techniques for ultrastructural characterization of the human papillary heart muscle cell in biopsy material. Virchows Arch [Pathol Anat] 410:265–279

Ericsson JLE, Brunk UT, Arborgh B (1978) Fixation. In: Johannessen JV (ed) Electron Microscopy in Human Medicine, vol 1, McGraw-Hill International Book Company, New York, p. 99

Ferrans VJ, Maron BJ, Buja LM, Ali N, Roberts WC (1975) Intranuclear glycogen deposists in human cardiac muscle cells: Ultrastructure and cytochemistry. J Molec Cell Cardiol 7:373–386

Ferrans VJ, Morrow AG, Roberts WC (1972) Myocardial ultrastructure in idiopathic hypertrophic subaortic stenosis. A study of operatively exised left ventricular outflow tract muscle in 14 patients. Circulation 45:769–792

Ferrans VJ, Roberts WC (1973) Intermyofibrillar and nuclear-myofibrillar connections in human and canine myocardium. An ultrastructural study. J Mole Cell Cardiol 5:247–257

Forbes MS, Sperelakis N (1976) The presence of transverse and axial tubules in the ventricular myocardium of embryonic and neonatal guinea pigs. Cell Tissue Res 166:83–90

Forbes MS, Sperelakis N (1980) Structures located at the levels of the Z-bands in mouse ventricular myocardial cells. Tissue & Cell 12:467–489

Forbes MS, Sperelakis N (1983) The membrane systems and cytoskeletal elements of mammalian myocardial cells. In: Dowben RM, Shay JW (eds) Cell and Muscle Mobility, vol. 3. Plenum Press, New York, p. 89

Forbes MS, Sperelakis N (1984) Ultrastructure of the mammalian cardiac muscle. In: Sperelakis N (ed) Function of the Heart in Normal and Pathological States. Martinus Nijhoff, The Hague, p. 3

Gabella G (1978) Inpocketings of the cell membrane (caveolae) in the rat myocardium. J Ultrastruct Res 65:135–147

Goldstein MA, Entman ML (1979) Microtubules in mammalian heart muscle. J Cell Biol 80:183–195

Goldstein MA, Sordahl LA, Schwartz A (1974) Ultrastructural analysis of left ventricular hypertrophy in rabbits. J Mol Cell Cardiol 6:265–273

Jones M, Ferrans VJ (1979) Myocardial ultrastructure in children and adults with congenital heart disease. In: Roberts WC (ed) Congenital Heart Disease in Adults. F.A. Davis Company, Philadelphia, p. 501

Kajihara H, Taguchi K, Hara H, Iijima S (1973) Electron microscopic observation of human hypertrophied myocardium. Acta Pathol Jpn 23:335–347

Kawamura K (1982) Cardiac hypertrophy. Scanned architecture, ultrastructure and cytochemistry of myocardial cells. Jpn Circ J 46:1012–1030

Koobs DH, Schultz RL, Jutzy RV (1978) Origin of lipofuscin and possible consequences to myocardium. Arch Pathol Lab Med 102:66–68

Laks MM, Morady F, Adomian GE, Swan HJC (1970) Presence of widened and multiple intercalated discs in the hypertrophied canine heart. Circ Res 27:391–402

Lazarides E (1980) Intermediate filaments as mechanical integrators of cellular space. Nature 283:249–256

Legato MJ (1970) Sarcomerogenesis in human myocardium. J Mol Cell Cardiol 1:425–437

Legato MJ, Mulieri LA, Alpert NR (1984) The ultrastructure of myocardial hypertrophy: Why does the compensated heart fail? Eur Heart J 5 (Suppl. F):251–269

Levin KR, Page E (1980) Quantitative studies on plasmalemmal folds and caveola of rabbit ventricular myocardial cells. Circ Res 46:244–255

Luftig RB, McMillan PN, Weatherbee JA, Weihing RR (1977) Increased visualization of microtubules by an improved fixation procedure. J Histochem Cytochem 25:175–187

Maron BJ, Ferrans VJ (1973) Significance of multiple intercalated discs in hypertrophied human myocardium. Am J Pathol 73:81–96

Maron BJ, Ferrans VJ (1974) Aggregates of tubules in human cardiac muscle cells. J Molec Cell Cardiol 6:249–264

Maron BJ, Ferrans VJ (1978) Ultrastructural features of hypertrophied human ventricular myocardium. Prog Cardiovasc Dis 21:207–238

Maron BJ, Ferrans VJ, Roberts WC (1975a) Myocardial ultrastructure in patients with chronic aortic valve disease. Am J Cardiol 35:725–739

Maron BJ, Ferrans VJ, Roberts WC (1975b) Ultrastructural

features of degenerated cardiac muscle cells in patients with cardiac hypertrophy. Am J Pathol 79:387–434

Orenstein J, Hogan D, Bloom S (1980) Surface cables of cardiac myocytes. J Molec Cell Cardiol 12:771–780

Prescott L, Brightman MW (1976) The sarcolemma of Aplysia smooth muscle in freeze-fracture preparations. Tissue & Cell 8:241–258

Robinson TF, Cohen-Gould L, Factor SM (1983) Skeletal framework in mammalian heart muscle. Arrangement of inter- and pericellular connective tissue structures. Lab Invest 49:482–498

Robinson TF, Winegrad S (1981) A variety of intercellular connections in heart muscle. J Molec Cell Cardiol 13:185–195

Roth LE (1967) Electron microscopy of mitosis in amebae. III. Cold and urea treatments: A basis for tests of direct effects of mitotic inhibitors on microtubule formation. J Cell Biol 34:47–59

Schaper J, Schwarz F, Hehrlein F (1981) Ultrastrukturelle Veränderungen im menschlichen Myocard bei Hypertrophie durch Aortenklappenfehler und deren Beziehung zur linksventrikulären Masse und Auswurffraktion. Herz 6:217–225

Sommer JR, Johnson EA (1979) Ultrastructure of the cardiac muscle. In: Berne RM, Sperelakis N, Geiger SR (eds) Handbook of Physiology. Section 2: The Cardiovascular System, vol. I: The Heart American Physiological Society, Bethesda, p 113

Sætersdal TS, Myklebust R, Skagseth E, Engedal H (1976) Ultrastructural studies on the growth of filaments and sarcomeres in mechanically overloaded human hearts. Virch Arch [Cell Pathol] 21:91–112

Thiéry G, Bergeron M (1976) Morphologie spatiale des mitochondries des tubes proximaux et distaux du néphron. Rev Can Biol 35:211–216

Tilney LG, Porter KR (1967) Studies on the microtubules in heliozea. II. The effect of low temperature on these structures in the formation and maintance of the axopodia. J Cell Biol 34:327–343

Travis DF, Travis A (1972) Ultrastructural changes in the left ventricular rat myocardial cells with age. J Ultrastruct Res 39:124–148

Van Noorden S, Olsen EGJ, Pearse AGE (1971) Hypertrophic obstructive cardiomyopathy, a histological, histochemical, and ultrastructural study of biopsy material. Cardiovasc Res 5:118–131

Accepted August 18, 1986